AGU PUBLICATIONS

JGR

Journal of Geophysical Research: Space Physics

RESEARCH ARTICLE
10.1002/2015JA022214

Key Points:
- The 17 March 2015 St. Patrick´s day geomagnetic storm
- Extreme ionospheric space weather event over the Brazilian sector
- Anomalous behavior in EIA during main phase and recovery phases

Supporting Information:
- Supporting Information S1
- Movie S1
- Movie S2
- Movie S3

Correspondence to:
P. R. Fagundes,
fagundes@univap.br

Citation:
Fagundes, P. R., F. A. Cardoso, B. G. Fejer, K. Venkatesh, B. A. G. Ribeiro, and V. G. Pillat (2016), Positive and negative GPS-TEC ionospheric storm effects during the extreme space weather event of March 2015 over the Brazilian sector, *J. Geophys. Res. Space Physics*, *121*, 5613–5625, doi:10.1002/2015JA022214.

Received 30 NOV 2015
Accepted 15 MAY 2016
Accepted article online 18 MAY 2016
Published online 11 JUN 2016

Positive and negative GPS-TEC ionospheric storm effects during the extreme space weather event of March 2015 over the Brazilian sector

P. R. Fagundes[1], F. A. Cardoso[1], B. G. Fejer[2], K. Venkatesh[1], B. A. G. Ribeiro[1], and V. G. Pillat[1]

[1]Physics and Astronomy Laboratory, Universidade do Vale do Paraiba, Sao Jose dos Campos, Sao Paulo, Brazil, [2]Center for Atmospheric and Space Sciences, Utah State University, Logan, Utah, USA

Abstract We studied the response of the ionosphere (*F* region) in the Brazilian sector during extreme space weather event of 17 March 2015 using a large network of 102 GPS- total electron content (TEC) stations. It is observed that the vertical total electron content (VTEC) was severely disturbed during the storm main and recovery phases. A wavelike oscillation with three peaks was observed in the TEC diurnal variation from equator to low latitudes during the storm main phase on 17–18 March 2015. The latitudinal extent of the wavelike oscillation peaks decreased from the beginning of the main phase toward the recovery phase. The first peak extended from beyond 0°S to 30°S, the second occurred from 6°S to 25°S, whereas the third diurnal peaks was confined from 13°S to 25°S. In addition, a strong negative phase in VTEC variations was observed during the recovery phase on 18–19 March 2015. This ionospheric negative phase was stronger at low latitudes than in the equatorial region. Also, two latitudinal chains of GPS-TEC stations from equatorial region to low latitudes in the east and west Brazilian sectors are used to investigate the storm time behavior of the equatorial ionization anomaly (EIA) in the east and west Brazilian sectors. We observed an anomalous behavior in EIA caused by the wavelike oscillations during the storm main phase on 17 March, and suppression of the EIA, resulting from the negative phase in VTEC, in the storm recovery phase.

1. Introduction

The response of the ionosphere-thermosphere system to geomagnetic storms is one of the important topics in space weather effects. As described in *Schunk and Sojka* [1996], geomagnetic storms occur when there is a large sudden increase in the solar wind speed. They can be particularly strong when the increased solar wind speed is accompanied by a large southward interplanetary magnetic field (IMF) component. Following a sudden storm commencement (SSC), there are growth, main, and recovery phases, respectively. During the growth phase, the magnetospheric electric field and particle precipitation patterns expand, the electric fields become stronger, and precipitation becomes more intense. During this phase, the Joule and particle heating rates and the electrojet currents increase. The energy input to the upper atmosphere maximizes during the main phase, while during the recovery phase the geomagnetic activity and energy input decrease. For large storms, the density, composition, and circulation of the ionosphere-thermosphere system can be significantly modified on a global scale and the modifications can persist for several days after the geomagnetic activity ceases. If the electron density increases as a result of storm dynamics, it is called a "positive ionospheric storm," while a decrease in electron density is called a "negative ionospheric storm." The mechanisms to explain the positive ionospheric storm involves the following: (a) an increases in the oxygen density, (b) changes in the meridional winds leading the ionosphere to higher altitude where the recombination rates are lower, (c) eastward electric field that uplifts the ionosphere as well as leads the ionosphere to regions of lower recombination rates, (d) downward protonospheric plasma fluxes, (e) traveling ionospheric disturbances (TIDs), and (f) plasma redistribution due to disturbed electric fields. On the other hand, negative storm phase is caused by changes in neutral composition that leads to decrease in the O/N_2 density ratio due to atmospheric disturbances [*Goncharenko et al.*, 2007; *Huang et al.*, 2005; *de Abreu et al.*, 2010, 2014].

The availability of extensive ground-based multisite observations and multiinstruments (all-sky imagers, Fabry-Perot interferometer, ionosonde, radar, TEC-GPS, etc.) facilitate to study the ionospheric response to geomagnetic storms with more insight [*de Abreu et al.*, 2010, 2011, 2014; *de Jesus et al.*, 2012, 2013; *Sahai et al.*, 2012; *Zhang et al.*, 2015] along with the fully coupled global ionosphere-thermosphere models [*Crowley et al.*, 2006; *Fuller-Rowell et al.*, 2007; *Lu et al.*, 2014; *Klimenko et al.*, 2011; *Sahai et al.*, 2011]. The

use of total electron content (TEC) measurements from dual frequency GPS receivers around the globe becomes a very powerful technique for ionospheric studies [*Fagundes et al*., 2015; *Olawepo et al*., 2015].

As mentioned by *Sahai et al*. [2011] and *de Jesus et al*. [2013], the ionospheric response is rather complicated and it is an important issue related with the space weather studies. The ionospheric response due to geomagnetic storms in the Brazilian sector has been studied by several investigators [*Abdu et al*., 2009, 2014; *Basu et al*., 2007; *Batista et al*., 2006, 2012; *Becker-Guedes et al*., 2004, 2007; *de Abreu et al*., 2011, 2014; *de Jesus et al*., 2010, 2012, 2013; *Klimenko et al*., 2011; *Sahai et al*., 2004, 2009a, 2009b], and the ionospheric response for each event showed different characteristics. Therefore, the investigation of individual cases is still important to understand the ionospheric behavior under extreme space weather events.

Abdu [1997] mentioned that the changes in ionospheric heights at low latitudes are produced by vertical plasma drifts driven by (a) magnetospheric electric fields penetrating to equatorial region, (b) disturbance dynamo electric fields, (c) disturbance meridional winds, and (d) disturbance zonal winds which are important only near sunset. *Fejer et al*. [2008] investigated the seasonal dependence of longitudinally averaged equatorial prompt penetration electric field (PPEF) and disturbance dynamo vertical drifts. They found that prompt penetration drifts are mostly upward and downward during nighttime and daytime in all seasons, respectively. Also, magnetospheric substorms may induce an eastward electric field in the day side of equatorial ionosphere when the IMF is southward [*Huang*, 2012].

In this paper, we present and discuss the ionospheric response in the Brazilian sector due to the largest geomagnetic storm of solar cycle 24 that occurred on 17 March 2015, where the minimum *Dst* index reached −223 nT at 23:00 UT. According to *Kataoka et al*. [2015], during this storm, the GOES satellites observed geosynchronous magnetopause crossings at 15:00–17:00 UT due to the strong compression of the magnetosphere. The storm main phase had two-step development. A halo coronal mass ejection (CME) associated with a C9.1 flare at 02:00 UT on 15 March 2015 was the main driver of the storm, while the shock and the sheath regions also played an additional role to cause the sudden commencement and the first step of the main phase, respectively. *Astafyeva et al*. [2015] have noticed most significant ionospheric changes at low latitudes in the American and eastern Pacific regions along with the hemispheric asymmetry in ionospheric response during this extreme event. This strong geomagnetic storm has a joint effect of the CME cloud arrival as well as the coronal hole high-speed streams. This storm is also characterized with a long and intense southward interplanetary magnetic field (−18 nT for 12 h) with a high *Kp* of "8−." Thus, investigating this storm is a great opportunity to improve our understandings on the storm time disturbances in magnetosphere, ionosphere, and thermospheric systems.

The present study using 102 GPS-TEC stations over Brazil show quite clearly that a strong positive and a negative ionospheric storm effects took place during the main and recovery phases of the geomagnetic storm, respectively. The disturbances in VTEC during the main phase were observed during daytime and post sunset time. However, the positive ionospheric storm presented unique pulse-mode characteristics, increase and decrease in the VTEC values, and this feature produce a wave-like TEC oscillation. Therefore, the equatorial ionization anomaly (EIA) during the main and recovery phases was severely disturbed. Also, the longitudinal differences in the ionospheric response to the geomagnetic storm are presented using two different latitudinal chains of receivers over the Brazilian east and west sectors.

2. Data Analysis and Observation

The intense geomagnetic storm of 17 March 2015 was one of the strongest storms of the solar cycle 24 and has been called St. Patrick's day geomagnetic storm. In this paper we present and discuss the results using simultaneous VTEC data from 102 GPS-TEC stations over Brazil The geomagnetic indices and solar wind parameters observed from 16 to 20 March 2015 are shown in Figure 1a (http://wdc.kugi.kyoto-u.ac.jp/, http://omniweb.gsfc.nasa.gov/form/omni_min.html). During this geomagnetic event, the sudden storm commencements (SSC) occurred on 04.45 UT on 17 March, and the *Dst* index reached maximum value of +56 nT on 17 March at 06:00 UT during the main phase and a minimum value of −223 nT on 17 March at 23:00 UT. The recovery phase started on 18 March and lasted for few days. Figure 1a shows that the IMF-B_z turned southward in two steps, the first incursion was short lived with a time duration of 4 h (17 March from 6:00 to 10:00 UT). Afterward, the IMF-B_z has become northward for 2 h followed by the second IMF-B_z southward incursion which lasted for 16 h from 17 March at 13:00 to 18 March at 5:00 UT Figure 1b shows

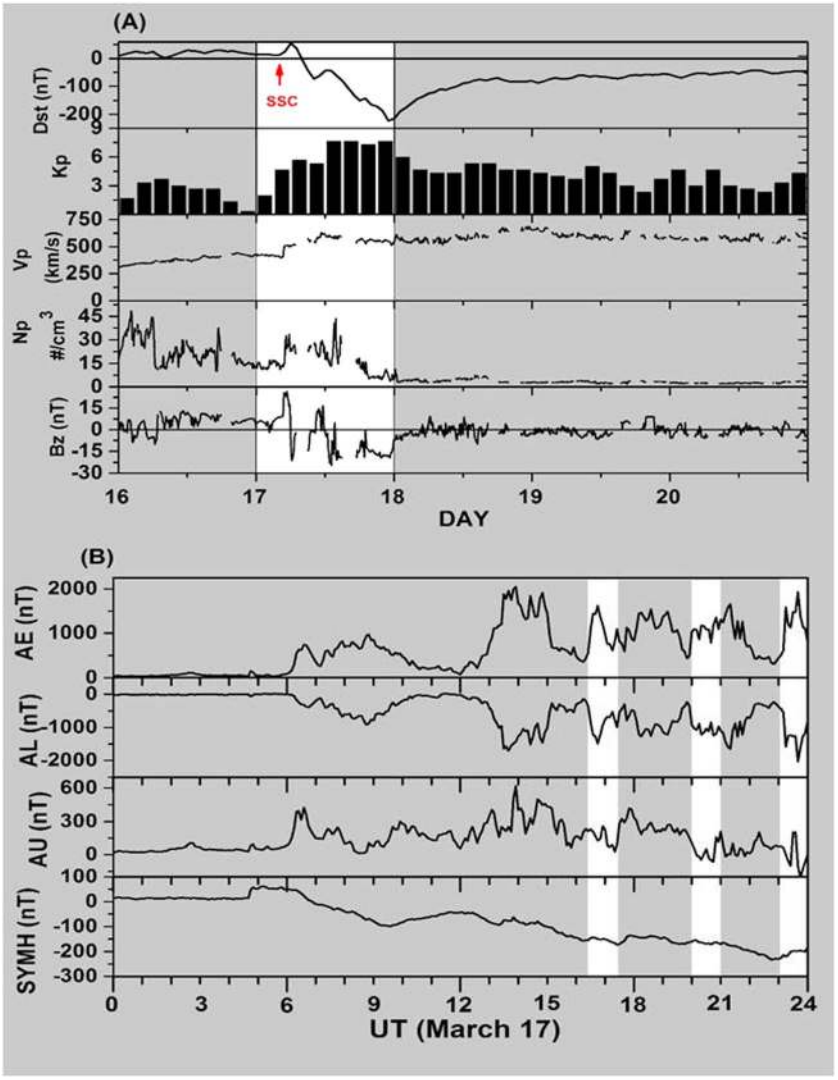

Figure 1. (a) Geomagnetic indices *Dst* and *Kp*, solar wind speed (*Vp*) and proton density per cm^3 (*Np*), and interplanetary vertical magnetic field component (B_z), observed from 16 to 25 March 2015. The white rectangle highlights the storm main phase. (b) *AE*, *AL*, *AU*, and *SYMH* indices during the main phase. The white rectangles denote the periods of positive ionospheric storm effects.

the *AE*, *AU*, *AL*, and *SYMH* index variations during the storm main phase. The white rectangles highlight the periods when the VTEC showed positive ionospheric storm peaks

The rapidly increasing number of dual frequency GPS receivers (more than 100) over the Brazilian region made it possible to study the ionosphere response to space weather events with more details compared with the earlier studies. These receivers were installed by the IBGE (Instituto Brasileiro de Geografia e Estatistica) and combined with large Brazilian territorial area which facilitated to study the ionospheric response in a wide range of 35°×30° of latitude and longitudes, respectively (see Figure 2). To study the TEC variations due to the present intense geomagnetic storm on 17 March 2015, 18 GPS stations at identified locations from north to south and east to west are considered. Figures 3a–3c show the VTEC contour plots for three different latitude regions (equatorial, low latitude, and beyond the EIA crest) and for the east and west sectors. The criteria adopted to choose the stations at equatorial region, low latitude, and beyond the EIA crest are as given below:

5°N ≤ dip latitude ≤ 5°S is equatorial region,
5°S < dip latitude < 20°S is low latitude, and
dip latitude ≥ 20°S is beyond the EIA region.

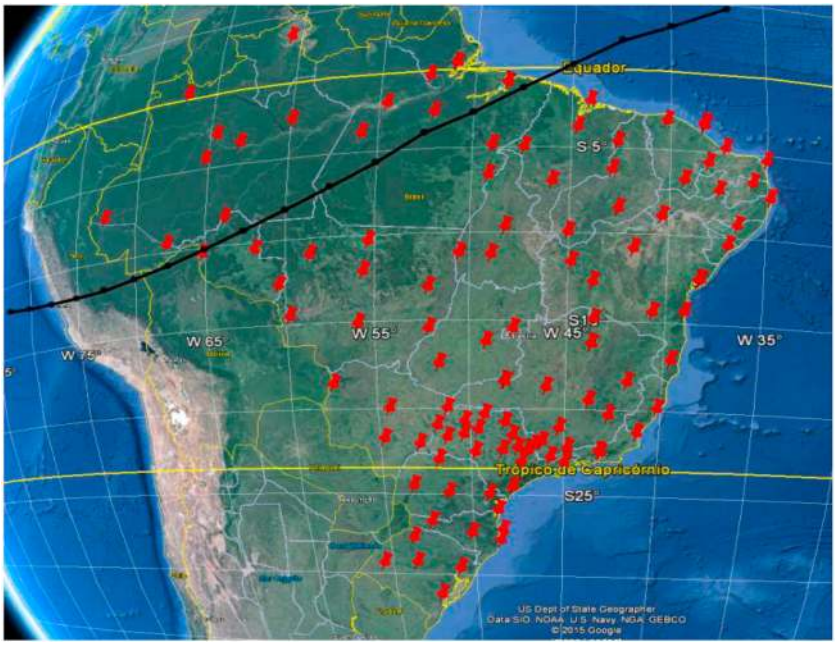

Figure 2. South American map showing the locations of the 102 GPS stations over Brazil used in the present investigation. The geographic and geomagnetic equators are shown in the map.

The VTEC plots in Figure 3 are presented as a function of universal time (UT) from 16 to 25 March. Each one of these Figures present six VTEC contour plots, where those in the first row of each panelrefer to east and the second row to west Brazilian sectors, respectively. In addition, the *Dst* index variations (solid black lines) is superimposed on the contour plots to highlight the VTEC variations during quiet time, main, and recovery storm phases. The details along with the coordinates about the 18 stations used in Figures 3a–3c are shown in Table 1.

The results presented in Figure 3a (equatorial stations) show the signatures of strong positive ionospheric storm (PIS), during the main phase (17 March), one peaking around 16:00–18:00 UT and a comparative weaker one around 19:00–21:00 UT. In addition, it can be noticed that the positive ionospheric storm peaks are stronger in the west sector than those in the east sector indicating the existence of longitudinal differences in the ionospheric response (Movie S1 in the supporting information).

The VTEC plots presented in Figure 3b for the low-latitude stations which are mostly affected by the geomagnetic storms very clearly indicates three strong positive ionospheric storm peaks during the main phase. These positive ionospheric storm peaks occurred between 16:00 and 18:00 UT, 19:00 and 21:00 UT, and 23:00 and 01:00 UT on 17 March 2015. It can also be noticed that the VTEC values in the west sector are larger than those in the east sector during the main phase.

From Figure 3c, the VTEC variations at the locations beyond the EIA crest show only one strong positive ionospheric storm peak around 16:00–18:00 UT. In this latitudinal region, noticeable differences are not observed in the positive ionospheric storm peak strength between the east and west sectors.

Therefore, the VTEC variations in Figures 3a–3c indicate that the positive ionospheric storm peaks are stronger in (bottom) the Brazilian west sector than those in the (top) Brazilian east sector for equatorial and low-latitude regions. The positive ionospheric storm peak that took place around 16:00–18:00 UT extends from equatorial region to beyond the EIA crest and the others were limited to the equatorial and low latitudes. Also, following the positive ionospheric effect in the main phase, a negative ionospheric storm (NIS) is noticed during the recovery phase on 18–19 March all over the Brazilian region (Movie S2 in the supporting information). In addition, the signatures of quasi 2 days planetary wave (Figures 3a–3c) can be seen in GPS-TEC at many equatorial and low-latitude stations. As discussed by *Fagundes et al*. [2009], the propagation of planetary waves are strongly affected by the short-time dominant perturbation related to very

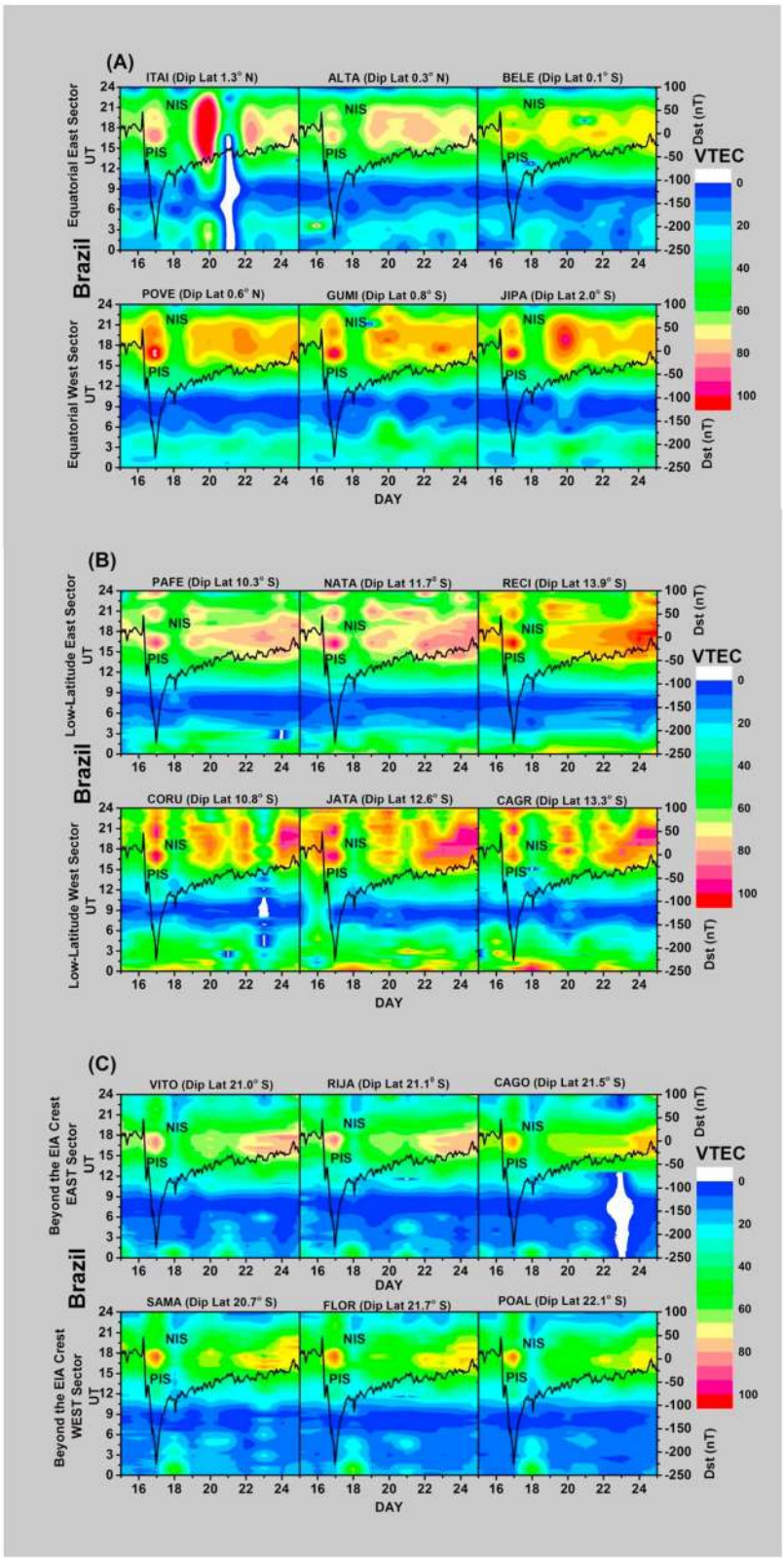

Figure 3. (a) VTEC variations with UT as a function of day of March (from 16 to 25) for six stations over Brazilian equatorial region. The three stations shown are representatives of the (top) east and (bottom) west sectors, respectively. (b) The same as Figure 3a but for low-latitude stations. (c) The same as Figure 3a but for the stations beyond the EIA crest. The black solid lines, PIS, and NIS are the *Dst* index variation, positive ionospheric storm, and negative ionospheric storm, respectively.

Table 1. Details of the GPS Stations Used in Figures 3a, 3b, 3c, 6b, and 6c With Names, Symbols, Latitudes, Longitudes, and Dip Latitude

GPS Station Name	Symbols	Geo. Lat. (+N)	Geo. Lon. (+W)	Dip. Lat. (+N)
		Equatorial Region		
Itaituba	ITAI	−4.3	56.0	1.3
Altamira	ALTA	−3.2	52.2	0.3
Belem	BELE	−1.4	48.5	−0.1
Porto Velho	POVE	−8.7	63.9	0.6
Guajara-Mirim	GUMI	−10.8	65.3	−0.8
Ji-Parana	JIPA	−10.9	62.0	−2.1
		Low-Latitude Region		
Pau dos Ferros	PAFE	−6.1	38.2	−10.3
Natal	NATA	−5.8	35.2	−11.7
Recife	RECI	−8.1	35.0	−13.9
Corumbá	CORU	−19.0	57.6	−10.8
Jataí	JATA	−17.9	51.7	−12.6
Campo Grande	CAGR	−20.4	54.5	−13.3
		Beyond EIA Crest Region		
Vitoria	VITO	−20.3	40.3	−21.0
Rio de Janeiro	RIJA	−22.8	43.3	−21.1
Campos Goytacazes	CAGO	−21.8	41.3	−21.5
Santa Maria	SAMA	−29.7	53.7	−20.7
Florianopolis	FLOR	−27.6	48.5	−21.7
Porto Alegre	POAL	−30.1	51.1	−22.1

intense geomagnetic storms, and after 2–4 days, the planetary waves signature become very clear again on ionospheric parameters. However, the interaction between planetary waves and geomagnetic storm perturbations is an interesting topic for further study.

As it is described above, the ionospheric (*F* region) response during the main and recovery phases from equator to beyond the EIA crest and from the east to the west Brazilian sectors (Figures 3a–3c) revealed some similarities and differences. Therefore, in order to highlight such similarities and differences, a comparison between disturbed days (red solid lines), averaged quiet day (black solid lines), and the averaged ±1 standard deviation (gray bands) are shown in Figures 4a and 4b. The quiet days used to calculate the mean values and standard deviation are from 7 to 15 March. Figures 4a and 4b are representative of Brazilian east and west sectors, respectively. The comparison between the VTEC daily averaged quiet day ±1 standard deviation (black solid line and gray band) and the VTEC disturbed period (red line) is very useful to highlight the occurrence of positive and negative ionospheric storm effects. When the red line (disturbed period) is above the gray band, then there is a positive ionospheric storm and on the contrary, we have negative ionospheric storm. The positive and negative ionospheric effects can be noted in Figures 4a and 4b (left and right), respectively.

Figures 4a and 4b show that during the main phase, the diurnal variations of TEC show wavelike oscillation from equator to beyond the EIA crest. The wavelike behavior is pronounced at low latitudes than those at equatorial region and beyond the EIA crest. However, it is also possible to see wavelike signatures at equatorial region and beyond the EIA crest. The first diurnal maximum took place on 17 March around 17:00 UT and is characterized by a positive ionospheric storm peak; the first maximum is indicated by vertical dashed lines in Figures 4a and 4b (left). This first diurnal maximum happened almost at the same time from equator to beyond the EIA crest and from east to west Brazilian sector, with different strengths. This indicates that this first positive ionospheric storm peak perturbation was clearly produced by a prompt penetration of electric field (PPEF) and not by traveling ionospheric disturbances (TIDs) or by any other sources. As mentioned by *Lima et al*. [2004] to distinguish if the positive ionospheric storm was produced by TID or electric field (*E* field), it is important to observe the positive ionospheric storm changes along the meridional direction. In case of TIDs, a meridional propagation of the disturbance wave with a phase and speed of about 100 to 400 m/s will be observed. Therefore, the perturbation occurs first beyond the EIA crest and sometime later at the low latitudes and finally at the equatorial region [*Lima et al*., 2004; *de Abreu et al*., 2010]. Whereas, with penetration of

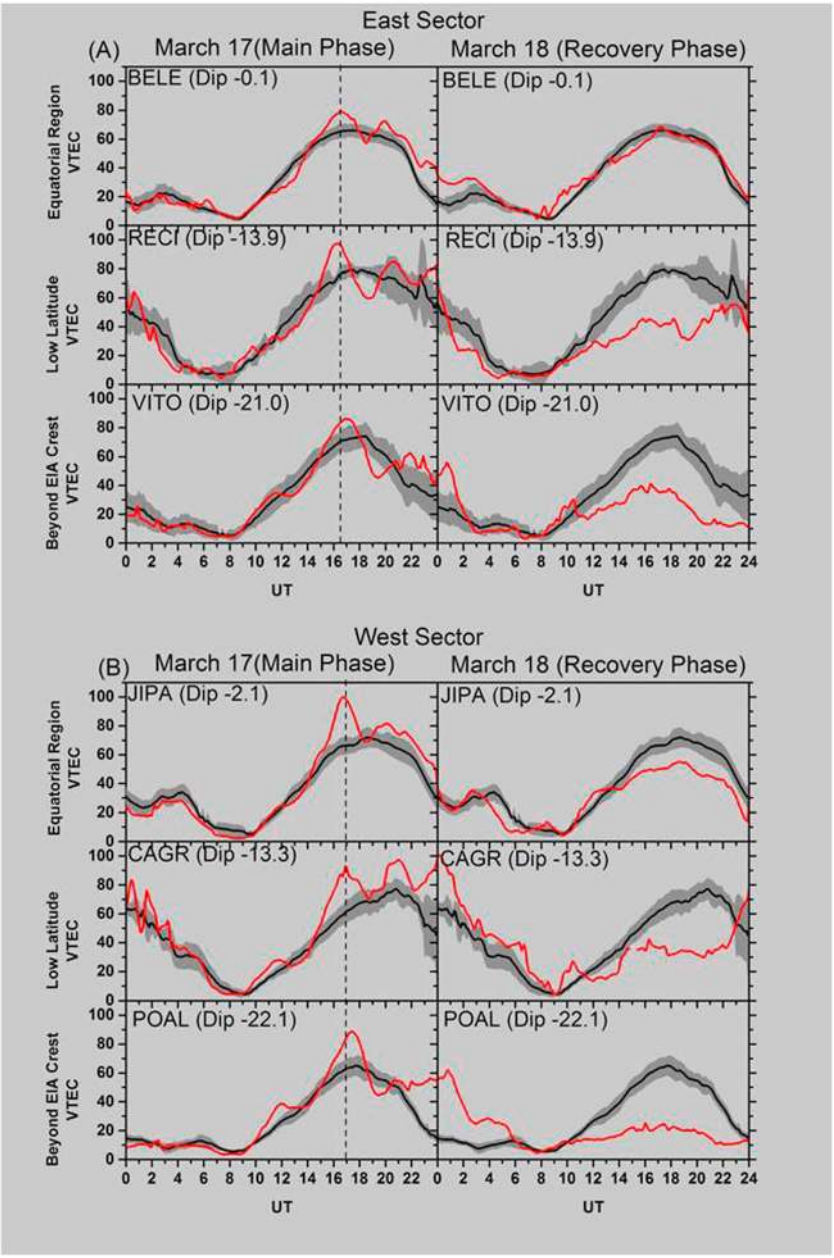

Figure 4. (a) The VTEC diurnal variations (red solid lines) for east Brazilian sector during main (17 March) and recovery (18 March) phases. The VTEC averaged quiet day and the averaged ±1 standard deviation are shown as black solid lines and as gray bands, respectively. (b) The same as Figure 4a but for west Brazilian sector. The vertical dashed lines indicate the first VTEC positive ionospheric storm around 17:00 UT.

the *E* field, the positive ionospheric storm perturbation must be simultaneous from low latitude to equatorial region, since *E* field penetration occurs on a global scale.

The second and third positive ionospheric storm peaks are not so strong and it is difficult to distinguish from Figures 4a and 4b whether they are due to *E* field or TID. However, using all 102 GPS stations, it was possible to produce regional maps, and from that, it is noticed that the second and third positive ionospheric storm peaks are not related with any TIDs (Figure 5). Note that Figure 4 shows better defined peaks away from the equator. This results from the fact that the low latitude and beyond the EIA regions are affected by prompt penetration electric fields directly as well as from the earlier equatorial plasma drift

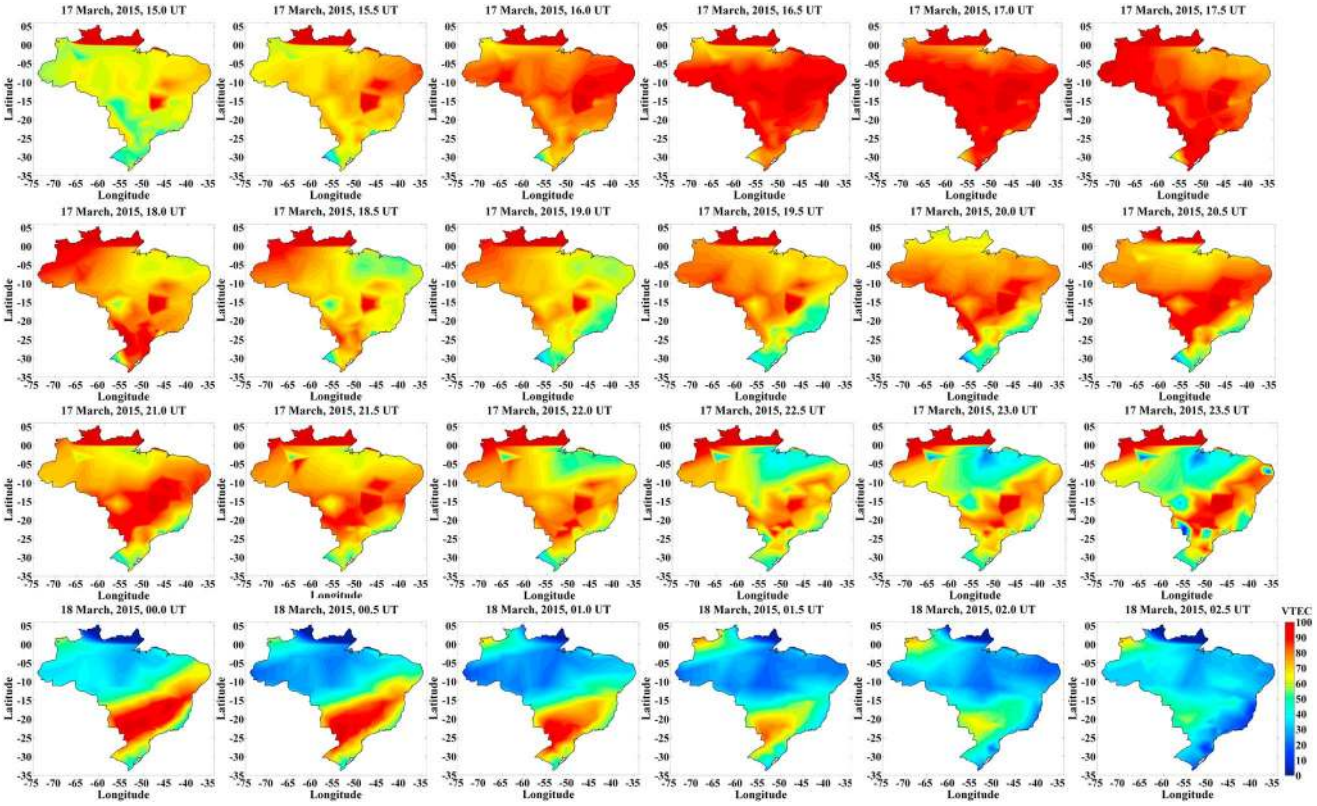

Figure 5. VTEC maps as a function of geographic longitude and latitude over Brazil obtained using 102 GPS-TEC stations. The maps are from 17 March 2015 at 15:00 UT to 18 March 2015 at 02:30 UT.

uplifts. This can be seen in Figure 4 which shows that the second density peak occurs first at the equator and slightly later at low and beyond the EIA region. This is a strong evidence that these peak were not due to TID effects since TID would cause changes first beyond the EIA region later in the low latitudes and finally at the equator.

It can also be mentioned here that the stations considered in the east and west Brazilian sectors are separated by around 20°—30°. Since this longitudinal distance is not very large, the *E* field disturbances reach the day time ionospheric sector at the same time with the same intensity and for similar duration. Hence, a marked longitudinal difference in the ionospheric response from these two sectors is not usually expected. Whereas in the present study, the TEC variations in the east and west sectors reveal that only the start and duration times were almost the same and the intensity have a marked difference. With the now available large network of more than 100 GPS-TEC receivers, in future, it will be possible to further investigate this feature with other geomagnetic storms.

During the first recovery day, a strong negative ionospheric storm is noticed in almost the whole Brazilian region, from equator to beyond the EIA crest. However, a few equatorial GPS stations at east sector do not show the negative ionospheric storm, such as Belem (see Figure 4a, upper right). This is also another example of marked longitudinal differences in the ionospheric response during this geomagnetic storm.

Figure 5 shows the VTEC regional maps as a function of geographic longitude and latitude over Brazil, obtained using 102 GPS-TEC stations (Figure 2 shows the locations of all 102 GPS stations). The maps present the VTEC changes with time during the storm main phase over Brazilian region from 17 March at 15:00 UT to 18 March at 02:30 UT (half an hour resolution). It is possible to see the increase of VTEC as well as its decrease from 16:00 UT to 17:30 UT from the equator to beyond the EIA crest. The first positive ionospheric storm was very strong and disturbed a large area. Also wavelike propagation is not noticed, suggesting that rapid VTEC changes are due to the substorm/PPFE (Movies S1–S3 in the supporting information).

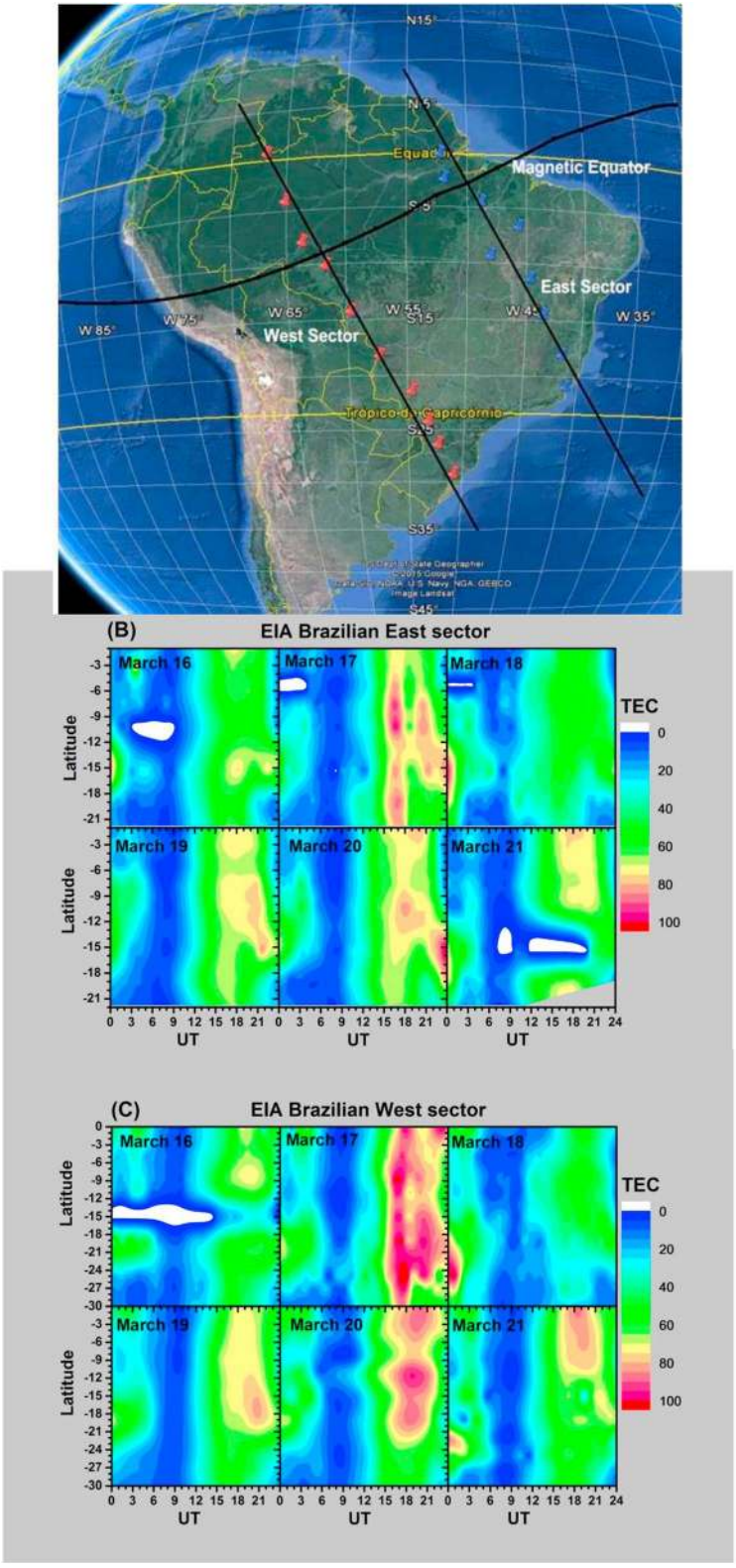

Figure 6. (a) Map showing the location of GPS stations used to study the EIA at east and west sectors. The GPS-TEC stations along of the black lines are used to investigate the EIA day-to-day changes in the east and west sectors. (b) Contour plots for the EIA east Brazilian sector showing the daily VTEC variation as a function of geographic latitude and UT from 15 to 20 March. The latitude starts from equator to the EIA crest in the southern hemisphere and beyond. (c) The same as Figure 4b but for west Brazilian sector.

The second and third positive ionospheric storm effects on VTEC are noticed from 20:00 UT to 21:30 UT and from 23:00 UT to 01:00 UT, respectively. As mentioned earlier, the other positive ionospheric storms are not as strong as the first positive ionospheric storm. Also, the second positive ionospheric storm was restricted to equatorial low latitudes, while the third positive ionospheric storm was restricted to low latitudes. However, it is clearly seen that neither of these disturbances are related with propagation of TIDs, since there are no wave propagation signatures from the observations.

In order to investigate the EIA behavior before and during the disturbed period, the VTEC data from two different longitudinal chains of GPS-TEC stations across the geomagnetic equator spanning the latitudes from equator to the beyond the EIA crest along east and west Brazilian sectors are considered (see Figure 6a and Table 1 for more details about GPS-TEC chains). Figures 6b and 6c show the day-to-day variations of EIA from 16 to 21 March in the east and west sectors, respectively.

During the main phase on 17–18 March (Figures 6b, east sector), it is seen that the EIA presented an unusual daytime behavior. Around 17:00 UT, the EIA extend from equatorial region to beyond the EIA crest, probably caused by a super fountain effect related with the PPEF. However, this super fountain effect time duration was very short (about 2 h) and suddenly the superfountain is suppressed for about 2 h. Afterwards, the EIA restores but it is not strong like the first one. Finally, during the post sunset time (around 24:00 UT), there is an enhancement in TEC beyond the crest which could be due to intensified electric field prereversal enhancement. Figure 6c (west sector) also presented a similar behavior that is seen in the east sector. But it appears that the geomagnetic storm was strong at this longitude and consequently the EIA was more disturbed than the east sector.

The observed disturbances in the EIA (both sectors) are time synchronized with positive ionospheric storm peaks and produce very clear signatures in the EIA daytime variations, more specifically between 16:00 UT on 17 March and 01:00 UT on 18 March. The first and strongest positive ionospheric storm peak produces a super fountain effect, and EIA extend from equator to beyond the EIA crest. It is strongly suggested that the EIA disturbances were triggered by eastward PPEF, and this PPEF leads to a super fountain effect that is seen on 17 March (Figures 6b and 6c, 17 March).

It is also important to mention that the EIA was completely suppressed during the first day of the recovery phase which is related with the VTEC depletion (Figures 6b and 6c, 18 March). Similar kind of features has been investigated during other geomagnetic storm events and it was attributed to the change in composition of the neutral gas which increases the N_2/O ratio [*de Jesus et al*., 2013]. *Astafyeva et al*. [2015] mentioned that the second IMF B_z (southward) event during the present geomagnetic storm lasted longer and caused more complex effects, including both positive and negative phases throughout all latitudes. In addition, they investigated the N_2/O ratio changes during this geomagnetic storm, using GUVI-TIMED satellite measurements, and confirmed a strong N_2/O composition changes.

3. Discussion and Conclusion

The 17–19 March 2015 geomagnetic storm was the strongest one that took place during the 24th solar cycle and the ionosphere was dramatically disturbed during a couple of days. During the main phase, there was positive ionospheric storm effect which presented unique characteristics of peaks that leads to increase and decreases in the VTEC. The increase and decreases in VTEC exhibit wavelike features (TID), especially at low latitude. However, as discussed by *de Abreu et al.* [2010] and *Lima et al.* [2004], the TID are generated at high latitude and travel toward the equatorial direction. The results presented in this study indicate that during the main phase, there are three positive ionospheric storm peaks at the same time indicating the absence of wave propagation characteristics (Figures 4 and 5). Therefore, it is strongly suggested that the wavelike oscillations were due to prompt penetration of electric field (PPEF) and not by the TIDs. Probably, an eastward *E* field penetrated at equatorial and low-latitude regions uplifts the *F* region where the recombination rates are lower leading to a positive ionospheric storm. These results indicate that in spite of the absence of more extensive equatorial electric field measurements (plasma drifts measurements), our data strongly suggest that prompt penetration electric fields were the main source of the equatorial plasma density enhancements.

The effect of PPEFs in the equatorial/low-latitude ionosphere could be associated with electric fields of solar/magnetospheric origin [*Wei et al*., 2015; *Huang,* 2012; *Fejer et al*., 2008; *Huang and Yumoto,* 2006] or associated

with magnetospheric dynamical process, such as substorms [*Huang*, 2012]. In both cases, there is a possibility to induce an eastward electric field and this eastward electric field uplift the *F* layer to higher altitudes where the recombination is much less and it results in an increase of *F* layer electron density/TEC (Figures 3, 4, and 5). It is interesting to mention here that to reinforce the idea of ionospheric disturbances caused by eastward PPEF during the main phase, *Astafyeva et al*. [2015] studied the polar cap index for this geomagnetic storm of March 2015. They noticed the first increase of the polar cap index at ~06:00 UT and at 09:00 UT and then four other intense polar cap index peaks at 14:00, 18:00, 21:00, and 23:30 UT on 17 March. Therefore, these substorms may be connected with the penetration of electric field in the Brazilian sector that leads the VTEC positive ionospheric peaks and consequently causing enormous day/evening time GPS-VTEC and EIA disturbances during the main phase.

During the observed positive ionospheric storm peaks, the AE and AL indices increase and decrease, respectively, almost simultaneously (Figure 1b). These changes suggest strong PPEF of the auroral electric field to low latitudes due to storm time substorm [*Fejer and Scherliess*, 1997]. Figure 1b (white rectangles) highlight the *AE* and *AL* (increase/decrease) when the VTEC showed positive ionospheric storm peaks. Also, there is a reduction of *ASY-H* index at the same time (Figure 1b, bottom), indicating the particle injection into ring current leading to the partial ring current intensification [*Ramsingh et al*., 2015]. In addition, *Ram et al*. [2016] and *Ramsingh et al*. [2015] investigated the ionosphere response due to St. Patrick's day storm on 17 March 2015 in the Indian and Indonesian sectors. They suggested that the *F* region disturbances during the main phase were produced by PPEF.

The equatorial ionization anomaly (EIA) was significantly disturbed during the main phase, and the signature of the positive ionospheric storm peaks are seen very clear in the EIA (Figure 6, 17 March). The first and strongest positive ionospheric storm peak (from 15:00 UT to 18:00 UT) induced a superfountain effect and consequently EIA intensified from equator to beyond the EIA crest. The second and third positive ionospheric storm peaks were not so strong, but it is possible to see their signatures on EIA in both Brazilian sectors. As suggested by many researchers, the superfountain effect during geomagnetic storms are closely related with PPEF and it leads to stronger EIA [*Lu et al*., 2013; *Sharma et al*., 2011; *Balan et al*., 2009; *Abdu et al*., 2007; *Batista et al*., 2006; *Mannucci et al*., 2005]. In the present study, it is also noted that the EIA west sector was more affected than the east sector by the PPEF, indicating the existence of significant longitudinal differences in the ionospheric response during this geomagnetic storm. It is important to mention that the VTEC from the equator to beyond EIA crest was much more disturbed in the west sector compared with the east sector, and therefore, it results into EIA longitudinal difference. However, it is important to mention that the VTEC during the storm main phase was positively disturbed in a wide longitudinal extension (~30°).

As far as we know, this is the first time to report that the equatorial ionization anomaly (EIA) in the east and west Brazilian sectors shows different response due to a PPEF (Figures 6b and 6c, 17 March). The EIA east-west (longitudinal) differences come as surprise because we do expected that the PPEF is more or less uniform within a range of 15°–20° in longitude. *Santos et al.* [2012] investigated that the ionospheric response due to a geomagnetic storm occurred in 21 January 2005 at Fortaleza (3.9°S, 38.45°W; dip angle −11.7°, Brazilian sector) and Jicamarca (12.0°S, 76.8°W; dip angle 0.64°, Peruvian sector), stations separated by more than 30° in longitude, and they found the *F* layer perturbation in both Brazilian and Peruvian sectors in South America due to PPEF. At Jicamarca, intensification in the equatorial eletroject irregularities and a strong increase of *F* layer height around midday were observed, but at Fortaleza, such features described above were not observed. In addition, the *F* layer at Fortaleza descends during the main phase (19:40 UT/16:40 LT on 21 January), but this feature was not observed at Jicamarca. The longitudinal differences found by *Santos et al.* [2012] are interesting, but we do expected some difference when we compare ionospheric data from equatorial region (Jicamarca) and low latitude (Fortaleza) during geomagnetic quiet and disturbed periods. On the other hand, the present investigation very clearly shows the EIA east-west differences using two chains of 10 GPS stations, each (from equator to beyond EIA crest). In Addition, different longitudinal ionospheric responses were investigated in different sectors such as American, Indian, African, and Asian [*de Abreu et al*., 2014; *Dmitriev et al*., 2013; *Horvath and Lovell*, 2014; *Sharma et al*., 2011; *Sahai et al*., 2009a, 2009b].

In 18 March 2015 (recovery phase), there was a strong negative ionospheric storm from equator to beyond EIA crest and from east to west sectors (Figures 3 and 4). Because of negative ionospheric storm, the EIA was suppressed and it is noticed that the suppression is quite similar in east and west Brazilian sectors. It

appears that the N_2/O ratio changes during the storm are similar over the Brazilian region. More details about the N_2/O ratio changes for this specific storm can be seen at *Astafyeva et al*. [2015].

The *F* layer response due to 17 March 2015 intense geomagnetic storm are studied using VTEC inferred from dual frequency GPS receivers over 102 stations covering a large area over Brazil. The 17 March 2015 storm is an extreme space weather event and it was one of the largest during the solar cycle 24. The main findings of the present investigation are summarized as follows:

1. There is a strong positive ionospheric effect during the storm main phase and a negative ionospheric effect during the recovery phase.
2. The positive ionospheric storms have three peaks and probably related with an eastward prompt penetration of electric field (PPEF) that uplifts the *F* region to the higher altitudes where recombination rates are lower. The positive ionospheric storm disturbed a wide longitudinal (~30°) and latitudinal (from equator to beyond the EIA crest) extents.
3. The equatorial ionospheric anomaly (EIA) is significantly disturbed by the geomagnetic storm (main phase).
4. A superfountain effect is noted in the equatorial ionospheric anomaly (EIA) from 15:00 UT to 18:00 UT. It is seen that the EIA extended from equator to beyond EIA crest. In addition, the EIA disturbance in the west sector is stronger than in the east sector, suggesting longitudinal differences in the ionospheric responses.
5. The first storm recovery day is characterized by a negative ionospheric storm caused by N_2/O ratio changes.
6. The negative ionospheric storm during the first recovery day completely suppresses the equatorial ionospheric anomaly.

Acknowledgments

We wish to express our sincere thanks to the Fundação de Amparo a Pesquisa do Estado de Sao Paulo for providing financial support through the process 2012/08445-9 and 2013/17380-0, CNPq grants 302927/2013-1 and 457129/2012-3, and FINEP 01.100661-00 for the partial financial support. The authors wish to express their sincere thanks to the IBGE (http://www.ibge.gov.br/home/geociencias/geodesia/rbmc/rbmc_est.php) for providing GPS-TEC data.

References

Abdu, M. A. (1997), Major phenomena of the equatorial ionosphere-thermosphere system under disturbed conditions, *J. Atmos. Sol. Terr. Phys.*, *59*(13), 1505–1519, doi:10.1016/S1364-6826(96)00152-6.

Abdu, M. A., T. Maruyama, I. S. Batista, S. Saito, and M. Nakamura (2007), Ionospheric responses to the October 2003 superstorm: Longitude/local time effects over equatorial low and middle latitudes, *J. Geophys. Res.*, *112*, A10306, doi:10.1029/2006JA012228.

Abdu, M. A., E. A. Kherani, I. S. Batista, and J. H. A. Sobral (2009), Equatorial evening prereversal vertical drift and spread *F* suppression by disturbance penetration electric fields, *Geophys. Res. Lett.*, *36*, L19103, doi:10.1029/2009GL039919.

Abdu, M. A., J. R. de Souza, I. S. Batista, A. M. Santos, J. H. A. Sobral, R. G. Rastogi, and H. Chandra (2014), The role of electric fields in sporadic *E* layer formation over low latitudes under quiet and magnetic storm conditions, *J. Atmos. Sol. Terr. Phys.*, *115*, 95–105, doi:10.1016/j.jastp.2013.12.003.

Astafyeva, E., I. Zakharenkova, and M. Förster (2015), Ionospheric response to the 2015 St. Patrick's day storm: A global multiinstrumental overview, *J. Geophys. Res. Space Physics*, *120*, 9023–9037, doi:10.1002/2015JA021629.

Balan, N., K. Shiokawa, Y. Otsuka, S. Watanabe, and G. J. Bailey (2009), Superplasma fountain and equatorial ionization anomaly during penetration electric field, *J. Geophys. Res.*, *114*, A03310, doi:10.1029/2008JA013768.

Basu, S., S. Basu, F. J. Rich, K. M. Groves, E. MacKenzie, C. Coker, Y. Sahai, P. R. Fagundes, and F. Becker-Guedes (2007), Response of the equatorial ionosphere at dusk to penetration electric fields during intense magnetic storms, *J. Geophys. Res.*, *112*, A08308, doi:10.1029/2006JA012192.

Batista, I. S., M. A. Abdu, J. R. Souza, F. Bertoni, M. T. Matsuoka, P. O. Camargo, and G. J. Bailey (2006), Unusual early morning development of the equatorial anomaly in the Brazilian sector during the Halloween magnetic storm, *J. Geophys. Res.*, *111*, A05307, doi:10.1029/2005JA011428.

Batista, I. S., M. A. Abdu, P. A. B. Nogueira, R. R. Paes, J. R. De Souza, B. W. Reinisch, and V. H. Rios (2012), Early morning enhancement in ionospheric electron density during intense magnetic storms, *Adv. Space Res.*, *49*(11), 1544–1552, doi:10.1016/j.asr.2012.01.006.

Becker-Guedes, F., Y. Sahai, P. R. Fagundes, W. L. C. Lima, V. G. Pillat, J. R. Abalde, and J. A. Bittencourt (2004), Geomagnetic storm and equatorial spread-F, *Ann. Geophys.*, *22*(9), 3231–3239, doi:10.5194/angeo-22-3231-2004.

Becker-Guedes, F., et al. (2007), The ionospheric response in the Brazilian sector during the super geomagnetic storm on 20 November 2003, *Ann. Geophys.*, *25*(4), 863–873, doi:10.5194/angeo-25-863-2007.

Crowley, G., et al. (2006), Global thermosphere-ionosphere response to onset of 20 November 2003 magnetic storm, *J. Geophys. Res.*, *111*, A10S18, doi:10.1029/2005JA011518.

de Abreu, A. J., et al. (2010), Hemispheric asymmetries in the ionospheric response observed in the American sector during an intense geomagnetic storm, *J. Geophys. Res.*, *115*, A12312, doi:10.1029/2010JA015661.

de Abreu, A. J., Y. Sahai, P. R. Fagundes, R. de Jesus, J. Á. Bittencourt, and V. G. Pillat (2011), An investigation of ionospheric *F* region response in the Brazilian sector to the supergeomagnetic storm of May 2005, *Adv. Space Res.*, *48*(7), 1211–1220, doi:10.1016/j.asr.2011.05.036.

de Abreu, A. J., P. R. Fagundes, M. Gende, O. S. Bolaji, R. de Jesus, and C. Brunini (2014), Investigation of ionospheric response to two moderate geomagnetic storms using GPS-TEC measurements in the South American and African sectors during the ascending phase of solar cycle 24, *Adv. Space Res.*, *53*(9), 1313–1328, doi:10.1016/j.asr.2014.02.011.

de Jesus, R., et al. (2010), Effects observed in the ionospheric *F* region in the South American sector during the intense geomagnetic storm of 14 December 2006, *Adv. Space Res.*, *46*(7), 909–920, doi:10.1016/j.asr.2010.04.031.

de Jesus, R., Y. Sahai, F. L. Guarnieri, P. R. Fagundes, A. J. de Abreu, J. A. Bittencourt, T. Nagatsuma, C. S. Huang, H. T. Lan, and V. G. Pillat (2012), Ionospheric response of equatorial and low latitude *F* region during the intense geomagnetic storm on 24–25 August 2005, *Adv. Space Res.*, *49*(3), 518–529, doi:10.1016/j.asr.2011.10.020.

de Jesus, R., Y. Sahai, P. R. Fagundes, A. J. de Abreu, C. Brunini, M. Gende, J. A. Bittencourt, J. R. Abalde, and V. G. Pillat (2013), Response of equatorial, low- and midlatitude *F* region in the American sector during the intense geomagnetic storm on 24-25 October 2011, *Adv. Space Res.*, *52*(1), 147–157, doi:10.1016/j.asr.2013.03.017.

Dmitriev, A. V., C. M. Huang, P. S. Brahmanandam, L. C. Chang, K. T. Chen, and L. C. Tsai (2013), Longitudinal variations of positive dayside ionospheric storms related to recurrent geomagnetic storms, *J. Geophys. Res. Space Physics*, *118*, 6806–6822, doi:10.1002/jgra.50575.

Fagundes, P. R., J. A. Bittencourt, J. R. Abalde, Y. Sahai, M. J. A. Bolzan, V. G. Pillat, and W. L. C. Lima (2009), *F* layer postsunset height rise due to electric field prereversal enhancement: 1. Traveling planetary wave ionospheric disturbance effects, *J. Geophys. Res.*, *114*, A12321, doi:10.1029/2009JA014390.

Fagundes, P. R., L. P. Goncharenko, A. J. de Abreu, K. Venkatesh, M. Pezzopane, R. de Jesus, M. Gende, A. J. Coster, and V. G. Pillat (2015), Ionospheric response to the 2009 sudden stratospheric warming over the equatorial, low, and middle latitudes in the South American sector, *J. Geophys. Res. Space Physics*, *120*, 7889–7902, doi:10.1002/2014JA020649.

Fejer, B. G., and L. Scherliess (1997), Empirical models of storm time equatorial zonal electric fields, *J. Geophys. Res.*, *102*(A11), 24,047–24,056, doi:10.1029/97JA02164.

Fejer, B. G., J. W. Jensen, and S. Y. Su (2008), Seasonal and longitudinal dependence of equatorial disturbance vertical plasma drifts, *Geophys. Res. Lett.*, *35*, L20106, doi:10.1029/2008GL035584.

Fuller-Rowell, T., M. Codrescu, N. Maruyama, M. Fedrizzi, E. Araujo-Pradere, S. Sazykin, and G. Bust (2007), Observed and modeled thermosphere and ionosphere response to superstorms, *Radio Sci.*, *42*, RS4S90, doi:10.1029/2005RS003392.

Goncharenko, L. P., J. C. Foster, A. J. Coster, C. Huang, N. Aponte, and L. J. Paxton (2007), Observations of a positive storm phase on 10 September 2005, *J. Atmos. Sol. Terr. Phys.*, *69*(10–11), 1253–1272, doi:10.1016/j.jastp.2006.09.011.

Horvath, I., and B. C. Lovell (2014), Perturbation electric fields and disturbance currents investigated during the 25 September 1998 great storm, *J. Geophys. Res. Space Physics*, *119*, 8483–8498, doi:10.1002/2014JA020480.

Huang, C. S. (2012), Statistical analysis of dayside equatorial ionospheric electric fields and electrojet currents produced by magnetospheric substorms during sawtooth events, *J. Geophys. Res.*, *117*, A02316, doi:10.1029/2011JA017398.

Huang, C. S., and K. Yumoto (2006), Quantification and hemispheric asymmetry of low-latitude geomagnetic disturbances caused by solar wind pressure enhancements, *J. Geophys. Res.*, *111*, A09316, doi:10.1029/2006JA011831.

Huang, C. S., J. C. Foster, L. P. Goncharenko, P. J. Erickson, W. Rideout, and A. J. Coster (2005), A strong positive phase of ionospheric storms observed by the Millstone Hill incoherent scatter radar and global GPS network, *J. Geophys. Res.*, *110*, A06303, doi:10.1029/2004JA010865.

Kataoka, R., D. Shiota, E. Kilpua, and K. Keika (2015), Pileup accident hypothesis of magnetic storm on 17 March 2015, *Geophys. Res. Lett.*, *42*, 5155–5161, doi:10.1002/2015GL064816.

Klimenko, M. V., V. V. Klimenko, K. G. Ratovsky, L. P. Goncharenko, Y. Sahai, P. R. Fagundes, R. de Jesus, A. J. de Abreu, and A. M. Vesnin (2011), Numerical modeling of ionospheric effects in the middle- and low-latitude *F* region during geomagnetic storm sequence of 9-14 September 2005, *Radio Sci.*, *46*, RS0D03, doi:10.1029/2010RS004590.

Lima, W. L. C., F. Becker-Guedes, Y. Sahai, P. R. Fagundes, J. R. Abalde, G. Crowley, and J. A. Bittencourt (2004), Response of the equatorial and low-latitude ionosphere during the space weather events of April 2002, *Ann. Geophys.*, *22*(9), 3211–3219, doi:10.5194/angeo-22-3211-2004.

Lu, G., J. D. Huba, and C. Valladares (2013), Modeling ionospheric superfountain effect based on the coupled TIME-GCM-SAMI3, *J. Geophys. Res. Space Physics*, *118*, 2527–2535, doi:10.1002/jgra.50256.

Lu, G., M. E. Hagan, K. Hausler, E. Doornbos, S. Bruinsma, B. J. Anderson, and H. Korth (2014), Global ionospheric and thermospheric response to the 5 April 2010 geomagnetic storm: An integrated data-model investigation, *J. Geophys. Res. Space Physics*, *119*, 10,358–10,375, doi:10.1002/2014JA020555.

Mannucci, A. J., B. T. Tsurutani, B. A. Iijima, A. Komjathy, A. Saito, W. D. Gonzalez, F. L. Guarnieri, J. U. Kozyra, and R. Skoug (2005), Dayside global ionospheric response to the major interplanetary events of 29–30 October 2003 "Halloween storms", *Geophys. Res. Lett.*, *32*, L12S02, doi:10.1029/2004GL021467.

Olawepo, A. O., O. A. Oladipo, J. O. Adeniyi, and P. H. Doherty (2015), TEC response at two equatorial stations in the African sector to geomagnetic storms, *Adv. Space Res.*, *56*(1), 19–27, doi:10.1016/j.asr.2015.03.029.

Ram, S. T., et al. (2016), Duskside enhancement of equatorial zonal electric field response to convection electric fields during the St. Patrick's day storm on 17 March 2015, *J. Geophys. Res. Space Physics*, *121*, 538–548, doi:10.1002/2015JA021932.

Ramsingh, S. Sripathi, S. Sreekumar, S. Banola, K. Emperumal, P. Tiwari, and B. S. Kumar (2015), Low-latitude ionosphere response to super geomagnetic storm of 17–18 March 2015: Results from a chain of ground-based observations over Indian sector, *J. Geophys. Res. Space Physics*, *120*, 10,864–10,882, doi:10.1002/2015JA021509.

Sahai, Y., P. R. Fagundes, J. R. Abalde, A. A. Pimenta, J. A. Bittencourt, Y. Otsuka, and V. H. Rios (2004), Generation of large-scale equatorial *F* region plasma depletions during low range spread-F season, *Ann. Geophys.*, *22*(1), 15–23.

Sahai, Y., et al. (2009a), Effects observed in the ionospheric *F* region in the east Asian sector during the intense geomagnetic disturbances in the early part of November 2004, *J. Geophys. Res.*, *114*, A00A18, doi:10.1029/2008JA013053.

Sahai, Y., et al. (2009b), Effects observed in the Latin American sector ionospheric *F* region during the intense geomagnetic disturbances in the early part of November 2004, *J. Geophys. Res.*, *114*, A00A19, doi:10.1029/2007JA013007.

Sahai, Y., et al. (2011), Studies of ionospheric *F* region response in the Latin American sector during the geomagnetic storm of 21–22 January 2005, *Ann. Geophys.*, *29*(5), 919–929, doi:10.5194/angeo-29-919-2011.

Sahai, Y., et al. (2012), Effects observed in the equatorial and low latitude ionospheric *F* region in the Brazilian sector during low solar activity geomagnetic storms and comparison with the COSMIC measurements, *Adv. Space Res.*, *50*(10), 1344–1351, doi:10.1016/j.asr.2012.07.006.

Santos, A. M., M. A. Abdu, J. H. A. Sobral, D. Koga, P. A. B. Nogueira, and C. M. N. Candido (2012), Strong longitudinal difference in ionospheric responses over Fortaleza (Brazil) and Jicamarca (Peru) during the January 2005 magnetic storm, dominated by northward IMF, *J. Geophys. Res.*, *117*, A08333, doi:10.1029/2012JA017604.

Schunk, R. W., and J. J. Sojka (1996), Ionosphere-thermosphere space weather issues, *J. Atmos. Sol. Terr. Phys.*, *58*(14), 1527–1574, doi:10.1016/0021-9169(96)00029-3.

Sharma, S., P. Galav, N. Dashora, and R. Pandey (2011), Longitudinal study of the ionospheric response to the geomagnetic storm of 15 May 2005 and manifestation of TADs, *Ann. Geophys.*, *29*(6), 1063–1070, doi:10.5194/angeo-29-1063-2011.

Wei, Y., B. Zhao, G. Guozhu, and W. Wan (2015), Electric field penetration into Earth's ionosphere: A brief review for 2000–2013, *Sci. Bull.*, *60*(8), 748–761, doi:10.1007/s11434-015-0749-4.

Zhang, S. R., et al. (2015), Thermospheric poleward wind surge at midlatitudes during great storm intervals, *Geophys. Res. Lett.*, *42*, 5132–5140, doi:10.1002/2015GL064836.